Computation of Minimum Energy Paths for Quasi-Linear Problems

Jeremy Chamard · Josef Otta · David J.B. Lloyd

Abstract We investigate minimum energy paths of the quasi-linear problem with the p-Laplacian operator and a double-well potential. We adapt the String method of E, Ren, and Vanden-Eijnden (J. Chem. Phys. 126, 2007) to locate saddle-type solutions. In one-dimension, the String method is shown to find a minimum energy path that can align along one-dimensional "ridges" of saddle-continua. We then apply the same method to locate saddle solutions and transition paths of the two-dimensional quasi-linear problem. The method developed is applicable to a general class of quasi-linear PDEs.

Keywords p-Laplacian · String method · Mountain pass algorithm

1 Introduction

Since the paper by Ambrosetti and Rabinowitz [2] in 1973, the mountain pass theorem has proved to be a major tool in nonlinear PDE analysis. Interest in mountain pass solutions continues to grow especially in the area of quasi-linear PDEs with Drábek *et al.* [12]. Correspondingly, the introduction of the mountain pass algorithm by Choi & McKenna [5] has lead to many new algorithms for computing saddle-point solutions of PDEs based on the linking theorem [8, 10, 21], providing insight for analysts working on nonlinear problems.

The quasi-linear bi-stable equation

$$\begin{cases} \varepsilon^p \Delta_p u - W'(u) = 0 & \text{in } \Omega, \\ \frac{\partial u}{\partial \nu} = 0 & \text{on } \partial\Omega, \end{cases} \qquad (1.1)$$

where $\varepsilon > 0$, Ω is a bounded domain in $\mathbb{R}^n$; $n \geq 1$, $W(u) = (1-u^2)^2$ is a symmetric double-well potential, $\Delta_p u = \text{div}(|\nabla u|^{p-2}\nabla u)$ is the p-Laplacian operator with $1 < p < \infty$ and

J. Chamard (✉) · D.J.B. Lloyd
Department of Mathematics, University of Surrey, Guildford GU2 7XH, UK
e-mail: j.chamard@surrey.ac.uk

J. Otta
Department of Mathematics, University of West Bohemia, Plzeň, Czech Republic

ν is the normal direction at the boundary, models a variety of nonlinear media such as phase transitions in water and ice at transition temperature [16], elasticity [1] and population models [23]. For $p > 2$, the p-Laplacian operator models degenerate slow-diffusion while for $p \in (1, 2)$ the operator describes singular fast diffusion.

Equation (1.1) is one of the simplest examples of degenerate elliptic equations since there is a loss of uniform ellipticity of the p-Laplacian operator when $|\nabla u| = 0$. Due to this degeneracy, it is known that solutions of (1.1) are only in general of class $C^{1,\alpha}(\Omega)$ for some $\alpha \in (0, 1)$; see [9]. Equation (1.1) may be reformulated as a variational problem by locating critical points of the energy functional

$$\mathcal{J}(u) = \int_{\Omega} \left[\frac{\varepsilon^p}{p} |\nabla u|^p + W(u) \right] d\mathbf{x}, \quad u \in W^{1,p}(\Omega). \tag{1.2}$$

For $p = 2$, the p-Laplacian operator reduces to the standard Laplacian and (1.1) becomes the well known semi-linear problem

$$\begin{cases} \varepsilon^2 \Delta u - W'(u) = 0 & \text{in } \Omega, \\ \frac{\partial u}{\partial \nu} = 0 & \text{on } \partial\Omega, \end{cases} \tag{1.3}$$

that has been extensively studied; see Kuzin & Pohozaev [20]. In this paper, we define $\nabla = (\partial_{x_1}, \ldots, \partial_{x_n})$ and $\mathcal{J}'$ to be the functional derivative of $\mathcal{J}$. For $p = 2$, one can show the existence of nontrivial solutions to (1.3) of saddle-type while the limit $\varepsilon \to 0$ has been extensively studied using Gamma Convergence techniques; see [22].

Otta [24] studied (1.1) in one-dimension with $\Omega = (0, 1)$ and Neumann boundary conditions using topological shooting techniques applied to equation (1.1), rewritten as a spatial dynamical system in x i.e.,

$$\begin{cases} u_x(x) = |v(x)|^{p'-2} v(x), \\ v_x(x) = \varepsilon^{-p} W'(u(x)), \end{cases} \tag{1.4}$$

where p and p' are conjugated exponents, i.e., $1/p + 1/p' = 1$ and $W(s) = |1 - s^2|^\alpha, \alpha > 1$. By considering the initial-value problem (1.4) with $(u, v)(0) = (u_0, 0)$, Otta was then able to use the results from Drábek *et al.* [11] to show that provided $|u_0| < 1$, there exists a unique periodic orbit. If $p > \alpha$ and $u_0 = \pm 1$ (i.e., the critical points of $W(s)$) then there is a loss of Lipschitz continuity of the right-hand side of (1.4). This loss of Lipschitz continuity leads to a loss of uniqueness of the initial-value problem and one can expect "finite-time" fronts to exist; fronts that attain $u = \pm 1$ in finite x as opposed to the Laplacian case when fronts connect $u(x) = \pm 1$ at $x = \pm\infty$. Figure 1, shows a sample of the possible solutions for the initial-value problem (1.4) when $p > \alpha$. The grey regions in Fig. 1 depict non-unique "dead-core" regions.

Drábek *et al.* [11] showed the existence of solutions for the parabolic system related to (1.1)

$$u_t = \varepsilon^p \Delta_p u - W'(u), \tag{1.5}$$

for α, $p > 1$ on $\Omega = (0, 1)$. For the stationary case of (1.5) with $p = 4$ and $W(s) = (1 - s^2)^2$ and sufficiently small ε, it was shown that the solutions are of saddle-type and form a whole continua of critical points in $W^{1,p}(\Omega)$. The continua is due to translations of the interfaces from $+1$ to -1 where the dimension of the continua manifold is determined by the number of transitions from $+1$ to -1 i.e., the continua is a one-dimensional curve if there exists monotonic fronts and two-dimensional if there exists transitions from $+1$ to -1 and back to $+1$. It is known that the number of transitions from $+1$ to -1 increases as ε is decreased.

Fig. 1 A selection of solutions of the initial-value problem (1.4) with $\alpha = 2$ and $p = 3$, $u(0) > 0$ and $v(0) = 0$. A continua of fronts (related by translations of the interface) connect ± 1. Periodic orbits exists for solutions $|u(0)| < 1$. All solutions with $|u(0)| > 1$ blow-up to infinity
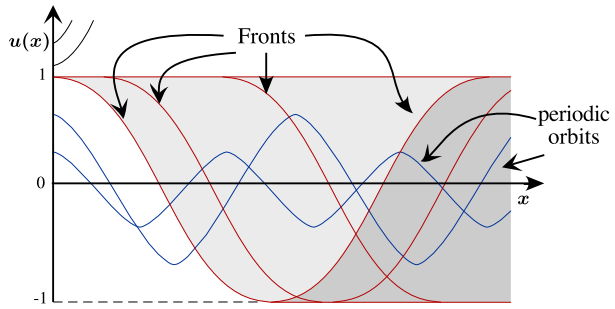
In higher dimensions, the existence of saddle-type solutions for (1.1) with Dirichlet and Neumann boundary conditions was proved by Otta [25]. However, it remains an open problem whether saddle-continua exist in higher dimensions.

To the best of the author's knowledge, there have been no attempts to numerically compute saddle-continua solutions of quasi-linear problems like (1.1). This appears to be a particularly tricky numerical problem since the usual approach to solving p-Laplacian type problems is to use nonlinear conjugate gradient methods due to the possible singular diffusion when $1 < p < 2$; see for example [3]. These methods are only able to compute minima of the energy functional (1.2) and will miss the saddle-type solutions we are trying to locate. Furthermore, to locate saddle-continua solutions, one would like to compute either a curve or surface of the continua. Hence, the standard Choi & McKenna algorithm [5] will be inappropriate for this task since the algorithm is designed to locate only one saddle-type solution. The High Linking algorithms [8] are only able to locate saddles of energy greater than an initial saddle making these algorithms unsuitable for the computation and detection of saddle-continua where they may have the same energy-value.

In the chemical physics literature, the location of saddles and transition paths in the context of calculating the stable configurations of molecules and chemical reaction paths have been extensively studied since the early 1940s; see Truhlar *et al.* [31] and references therein. One is interested in understanding the finite-dimensional energy landscape describing how molecules change from one state to another. Of crucial importance is the computation of the *Minimal Energy Path* (MEP) that provides the most likely transition path from one configuration to another and the corresponding *transition state* (saddle point); see [18]. In particular, the MEP can yield the likely transition dynamics of (1.5) in the presence of small noise.

The MEP $\gamma(t)$ is defined as

$$\nabla^{\perp} \mathcal{J}(\gamma(t)) = 0, \qquad (1.6)$$

where $\gamma \in C([0, 1], X)$, $X = \mathbb{R}^n$, $\mathcal{J}$ is the energy functional, and $\nabla^{\perp} \mathcal{J}$ is the steepest descent direction perpendicular to the path connecting the two stable configurations $\gamma(0)$ and $\gamma(1)$. Intuitively, one can think of the condition (1.6) as requiring the path to lie at the bottom of the "valleys" connecting $\gamma(0)$ and $\gamma(1)$.

Several numerical algorithms have been developed in order to compute MEPs and transition states. The two main algorithms are the Nudged Elastic Band (NEB) method [18] and the String method; see [13, 15]. The NEB method, considers the path connecting $\gamma(0)$ and $\gamma(1)$ as a piecewise connected path of springs. The NEB method then minimises both the condition (1.6) and the sum of the spring forces. The spring forces are required to prevent the path from "splitting" in two.

The String method [13] considers a continuous path connecting $\gamma(0)$ and $\gamma(1)$. The path is then discretised $\gamma(t_i) \approx \gamma_i$ for $i = 0 \ldots N - 1$ (where N is the number of points) and for
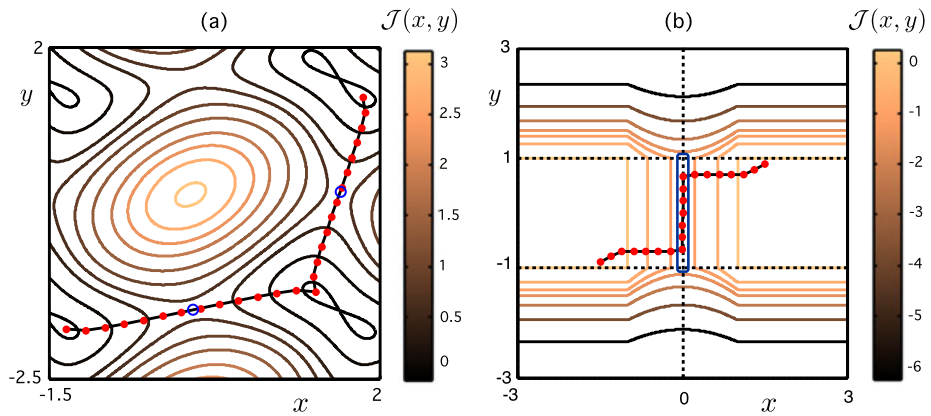
Fig. 2 A contour plot of the String method applied to (**a**) $\mathcal{J}(x, y) = \cos(2x) + 0.57 \cos(2x - 2y) + 2 \cos(2y) + 1$ with an initial endpoints at $(-0.5, -1.5)$ and $(1.5, 1)$ and (**b**) $\mathcal{J}(x, y) = \min(x^2, 1) - \max(y^2, 1)$, a surface that possesses a critical-point-continua, with an initial endpoints at $(-1.5, -0.9)$ and $(1.5, 0.9)$. The paths shown are minimum energy paths, and the initial paths consist of segments of equidistributed path points. In both *panels* the initial path for the String method is shown as a *dashed grey straight line*. We see that for both energy surfaces, the String method produces paths that pass through saddles. In particular, the path found in *panel (b)* passes along the ridge of saddle-continua at $x = 0$, $-1 \leq y \leq 1$

each point along the path the ODE

$$\frac{d\mathcal{J}[\gamma_i]}{d\tau} = \nabla^\perp \mathcal{J}[\gamma_i], \tag{1.7}$$

is stepped in τ (either using Euler's method or Runge-Kutta method). After each step in τ, the points along the path are equi-distributed with respect to arc-length to prevent path-splitting. Usually, the right-hand side of (1.7) is replaced with the gradient of the energy and the String method is then equivalent to carrying out steepest descent at each point along the path [15]; see Fig. 2(a) for an application of the String method to a two-dimensional energy surface.

We note that the MEPs obtained with the NEB and the String method do not guarantee that any of the computational points lie on a saddle. To acquire good saddle approximations one may either use the climbing image method [18] or Newton's method. Furthermore, solutions found by the NEB and string method depend greatly on the choice of the initial path, and in some cases an inadequate initial path can result in convergence failure. For example, if the whole path lies inside the basin of attraction of the same local minimum, then the whole path will converge to that minimum, and thus the method fails to locate any saddles.

The condition (1.6) has an interesting consequence for the computation of saddle-continua since MEPs will naturally want to follow along regions where $\mathcal{J}' = 0$ as much as possible. In Fig. 2(b), we show how the String method locates a continua of critical points for a two-dimensional energy surface $\mathcal{J}(x, y) = \max(x^2, 1) - \min(y^2, 1)$. This property of the String method does not appear to have been investigated before. We note that the String method is not guaranteed to locate saddle-continua. For instance, if the initial conditions of the path in Fig. 2(b) are horizontal, then the path will simply pass straight over the continua. Furthermore, the String method is only able to find continua of critical points that are pa-rameterised by a one-dimensional curve. However, our numerical investigations show that,

in general, if a saddle-continuum exists and the initial path is chosen wisely, then the String method can locate it.

The String method has been successfully applied to PDEs in the context of ferromagnetic thin films and current dissipation in thin superconducting wires [14, 26, 27]. In this paper, we propose an infinite-dimensional version of the String method that allows us to compute MEPs and continua of critical points of quasi-linear problems such as (4.1). We aim to consider MEPs with the space $X = W^{1,p}(\Omega)$ in (1.6).

The paper is outlined as follows. In Sect. 2, we present the numerical algorithms we use to investigate (1.1), where the String method is extended to the infinite-dimensional space $W^{1,p}(\Omega)$. We discuss the importance of the choice of the steepest descent vector in Sobolev space by considering $W^{1,p}(\Omega)$ as a completion of $C^\infty(\Omega)$ with respect to the standard $W^{1,p}(\Omega)$ Sobolev norm. We present our results in Sect. 3, and draw conclusions and discuss how our numerical methods can be applied to more general quasi-linear problems in Sect. 4.

2 Numerical Methods

2.1 The String Method

The version of the String method we shall use is by E *et al.* [13, 15]. This method has been shown to be robust and fast converging to the MEP. Given an energy functional $\mathcal{J}$, we let $u = u(x, t; \tau)$ be the position of the string where t is the parameterisation of the string and we evolve the following equation for a number of small timesteps:

$$\begin{cases} u_\tau(x, t; \tau) = D^*\mathcal{J}[u(x, t; \tau)], \\ u(x, t; 0) = u_0(x, t), \end{cases} \tag{2.1}$$

where $D^*\mathcal{J}[u(x, t; \tau)]$ is the steepest descent direction of the path at the point t and time τ.[1] If the path is discretized, then after each timestep we interpolate the path points so that they are equidistributed with respect to parametric arclength.

We note that other reparameterisations are possible with the most common choices being energy-weighted arc-length [13] or equi-distribution of error [28]. The reparameterisation of the path has strong links with moving meshes for the solution of parabolic partial differential equations [4].

A crucial step in the String method is the calculation of the steepest descent direction v. For this, we follow Choi & McKenna [5] and compute the steepest descent direction w of $\mathcal{J}$ at the point u such that the functional $\mathcal{J}$ has the largest decrease per unit norm. One can choose several different norms when computing the steepest descent. However, it is natural to look for the steepest descent direction in the space of solutions being sort. Thus, we wish to find

$$w := \min_{\|v\|_{1,q}=1} \mathcal{J}'(u)v, \tag{2.2}$$

where $v \in W^{1,q}(\Omega)$ and $\|\cdot\|_{1,q}$ is the standard Sobolev norm i.e.,

$$\|u\|_{1,q} = \left(\int_\Omega \left[|\nabla u|^q + |u|^q\right]d\mathbf{x}\right)^{1/q}.$$

---

[1]We call $D^*\mathcal{J}(u)$ the steepest descent of $\mathcal{J}$ at u if it exists, and $\mathcal{J}'(u)v$ the directional derivative of $\mathcal{J}(u)$ in the direction v.

Upon introducing the Lagrange functional L, we can reformulate this problem as a finding a critical point of

$$L(v, \lambda) := \mathcal{J}'(u)v + \lambda(\|v\|_{1,q}^q - 1),$$

$$= \int_\Omega \Big[\varepsilon^p |\nabla u|^{p-2} \nabla u \nabla v + W'(u)v \Big] d\mathbf{x} + \lambda \left(\int_\Omega \Big[|\nabla v|^q + |v|^q \Big] d\mathbf{x} - 1 \right).$$

By taking the Fréchet derivative of L, we compute the stationary point of L to yield

$$L'(v, \lambda)\varphi = \int_\Omega \Big[\varepsilon^p |\nabla u|^{p-2} \nabla u \nabla \varphi + W'(u)\varphi \Big] d\mathbf{x}$$

$$+ \lambda \left(\int_\Omega \Big[q|\nabla v|^{q-2} \nabla v \nabla \varphi + q|v|^{q-2} v\varphi \Big] d\mathbf{x} \right),$$

for all $\varphi \in W^{1,q}(\Omega)$. Thus, stationary points of $L(v, \lambda)$ corresponds to finding the weak solution of the following equation

$$\begin{cases} -\nabla \cdot (|\nabla z|^{q-2} \nabla z) + |z|^{q-2} z = \varepsilon^p \nabla \cdot (|\nabla u|^{p-2} \nabla u) - W'(u) & \text{in } \Omega, \\ \frac{\partial z}{\partial \nu} = 0 & \text{on } \partial\Omega, \end{cases} \quad (2.3)$$

where $z = (q\lambda)^{1/(q-1)} v$ and u is given. It is easy to show that $\lambda > 0$ and the function $v = z(q\lambda)^{1/(1-q)}$ defines the steepest descent direction in $W^{1,q}(\Omega)$.

The natural space to look for the steepest descent direction is in $W^{1,p}(\Omega)$ i.e., $q = p$. Existence of the steepest descent direction for $q = p$ and $p \in [2, \infty)$, defined by (2.3), follows since z also satisfies the equation

$$\int_\Omega \Big[\nabla z |\nabla z|^{p-2} \nabla \varphi + z|z|^{p-2} \varphi - f(\mathbf{x})\varphi \Big] d\mathbf{x} = 0, \quad \forall \varphi \in \mathcal{C}^\infty(\Omega),$$

where $f \in W^{-1,q}(\Omega)$ is the right-hand-side of (2.3), and the direct method of Calculus of variations can be applied; see Struwe [29, Theorem 1.3]. Uniqueness follows by the fact that the p-Laplacian operator is strongly monotone.

A key complication with looking for the steepest descent direction in $W^{1,p}(\Omega)$ is that one needs to solve the nonlinear PDE (2.3) if $p \neq 2$ for z. It may be computationally better to choose the steepest descent direction to be in $H^1(\Omega)$ i.e., $q = 2$, where one needs only solve a linear PDE for the steepest descent direction greatly speeding up the computation. One can not prove that the $H^1(\Omega)$ steepest descent exists since the right-hand side of (2.3) may not live in $H^{-1}(\Omega)$ for general $p \in (1, \infty)$, but the discretized $H^1(\Omega)$ steepest descent should be equivalent to the discretized $W^{1,p}(\Omega)$ steepest descent. Hence, we expect the $H^1(\Omega)$ steepest descent to allow us to locate saddle-point solutions of (1.1). The effect of choosing different norms for the steepest descent direction will be investigated in the following sections.

In order to numerically solve (2.3), we need to discretise the p-Laplacian operator. We choose two discretisations on the domains $\Omega = (0, 1)$ or $\Omega = (0, 1)^2$: Finite differences and Chebyshev pseudo-spectral method. We will use both methods to test convergence and compare with analytical results, cf. Otta [24].

We first describe the finite difference method. In one dimension, we impose a equi-spaced mesh $x_i = ih, h = 1/(N_x - 1)$ and $i = 0, \ldots, N_x - 1$ and approximate $u(x_i) \approx u_i$ and its derivatives via central difference approximations. In two dimensions, we employ the standard 5-point stencil on a uniform mesh for calculating the spatial derivatives. This scheme is

equivalent to the finite element discretisation using a union of regular triangles with piece-wise linear basis functions; see Choi & McKenna [5].

The second discretisation method we use is the Chebyshev pseudo-spectral method described in Trefethen [30]. In order to compute the 2D operator, we use a tensor product grid and calculate the discretised p-Laplacian operator using Kronecker products: if A is an $m \times n$ matrix and B is a $p \times q$ matrix, then the Kronecker product $A \otimes B$ is an $mp \times nq$ matrix which consists of $m \times n$ blocks where each block is a $p \times q$ matrix: the (i, j)th block is given by $a_{ij}B$. This approach yields the following approximation for the p-Laplacian operator

$$D_x = D_{N_x} \otimes I_{N_y},$$
$$D_y = I_{N_x} \otimes D_{N_y},$$
$$\nabla(|\nabla u|^{p-2}\nabla u) \approx D_x \left[(|D_x\tilde{u}|^2 + |D_y\tilde{u}|^2)^{(p-2)/2} D_x\tilde{u} \right]$$
$$+ D_y \left[(|D_x\tilde{u}|^2 + |D_y\tilde{u}|^2)^{(p-2)/2} D_y\tilde{u} \right],$$

where $\tilde{u}$ is the approximation of u on the tensor product grid, I_N is the identity matrix of size N, and D_N are the Chebyshev pseudo-spectral differentiation matrices of size N and, N_x and N_y are the number of modes used in the x and y direction, respectively; see [30].

The discretised form of (2.3) can be solved using either nonlinear conjugate gradient methods or nonlinear least square methods such as the trust-region or Levenberg-Marquardt method; see Barrett & Liu [3] for an application of the Polak-Ribiére conjugate gradient method applied to the p-Laplacian and Coleman & Li [7] for a description of the trust-region method. To impose the boundary conditions, we solve concurrently the discretised form of (1.1) on the interior of the domain and the boundary conditions.

To initialise the String method, we define an initial path $(u_s(t, \mathbf{x}))$ that is a piecewise convex combination of three functions $(\tilde{u}_1, s, \tilde{u}_2)$ that connect $\tilde{u}_1$ and $\tilde{u}_2$ via s such that

$$u_s(t, x) = \begin{cases} 2ts(\mathbf{x}) + (1 - 2t)\tilde{u}_1(\mathbf{x}), & t \in [0, \frac{1}{2}], \\ (2t - 1)\tilde{u}_2(\mathbf{x}) + (2 - 2t)s(\mathbf{x}), & t \in (\frac{1}{2}, 1]. \end{cases} \quad (2.4)$$

We usually take $\tilde{u}_1 \equiv 1$ and $\tilde{u}_2 \equiv -1$. Values of ± 1 correspond to the wells of the potential $W(u)$ since these are known trivial solutions to (1.1) but one can take more general functions. The function s determines the subspace of functions that we search for a saddle.

The String method is coded as the following algorithm:

Input: $\mathcal{J}$, $\tilde{u}_1$, s, $\tilde{u}_2$, *tol*, $h_{\max}$, N_{It}, N_t

1. Compute discrete initial path $u(t_i) \approx u_i$ where $t_i = i/N_t, i = 0, \ldots, N_t$. The path $U = \{u_1, u_2, \ldots, u_{N_t}\}$ is defined as a convex combination of $\tilde{u}_1$, s and $\tilde{u}_2$ by (2.4).
2. Reparametrize the path U to get points equidistantly distributed in $W^{1,p}(\Omega)$ norm.
3. Evaluate the steepest descent for all points in U by (2.3).
4. Minimize the path U in the steepest descent direction with constrained maximal step size by parameter $h_{\max}$.
5. Reparametrize the path to get equidistantly distributed points in $W^{1,p}(\Omega)$ norm.
6. Check whether $W^{1,p}(\Omega)$ norm of the movement of the string is less than the convergence tolerance *tol*, or if the number of iterations is more than N_{It}. If not, go to step 3.
7. Take the point on the path with the highest energy u_m.

Output: u, residuum of u and the critical-point approximation u_m.

Once a saddle point approximation has been located using the String method, we can either apply Newton's method or the climbing image method [18] to converge to the saddle point. One can also continue solutions of (1.1) using pseudo-arclength continuation to path-follow the solution as an equation parameter is varied to trace out bifurcation diagrams; see [19] and references therein.

2.2 Implementation

The String method and numerical continuation were implemented using MATLAB R2007b and R2009a with the nonlinear solver `fsolve`.

The computations were carried out on DRAGON, a dual core 2.7 GHz PowerPC G5 with 4 GB of RAM, and PHOENIX, a server with two 3 GHz dual core Xeon processors with 8 GB of RAM, both running Mac OS 10.5, and the Cluster DAMADAMA equipped with two Intel Xeon 5320 CPU 1.86 GHz - 2x4 cores with 16 GB of RAM running under Debian 4.0.

2.3 Convergence of Methods

The numerical computation of nonlinear diffusion problems is known to be a delicate topic, and so we carry out spatial convergence tests for our numerical discretisations of (1.1).

The two critical parameters governing convergence are p and ε. The parameter ε governs the sharpness of the interfaces. In particular, as $\varepsilon \to 0$ we expect u converges to discontinuous solutions in $BV([-1, 1])$. Hence, for small ε we have a sharper interface, and thus expect worse convergence.

Correspondingly, one may expect numerical difficulties when $p < 2$ since the term $|\nabla u|^{p-2}$ may become singular. Furthermore for large p, the nonlinear diffusion is enhanced also suggesting convergence may be difficult. This intuitive feel for how the convergence depends on p was proved by Barrett & Liu [3] (see also [6, 17]) for finite-element approximations of the p-Laplacian problem

$$-\nabla \cdot (|\nabla u|^{p-2}\nabla u) = f, \quad \text{in } \Omega \subset \mathbb{R}^2, \text{ and } u = g \text{ on } \partial\Omega. \tag{2.5}$$

The authors considered a regular triangular finite-element discretisation (akin to a 5-point finite-difference approximation) on a uniform mesh of step size h. If u is only in $W_0^{1,p}(\Omega) \cap W^{2,p}(\Omega)$, reference [6] gives the error bound

$$\|u - u^h\|_{1,p} \leq \begin{cases} Ch^{p/2} & \text{if } p \leq 2, \\ Ch^{2/p} & \text{if } p \geq 2. \end{cases} \tag{2.6}$$

Under additional regularity assumptions, Barrett & Liu [3] were able to prove more optimal error bounds. In particular, provided that $u \in W^{3,1}(\Omega) \cap C^{2,(2-p)/p}(\overline{\Omega})$ and $p \in (1, 2)$, they were able to show that the error bound is $\mathcal{O}(h)$ and in the case $p > 2$ if $u \in W^{1,\infty}(\Omega) \cap W^{2,2}(\Omega)$ then the second error bound in (2.6) still holds.

Barrett & Liu also carried out several numerical experiments of the radially symmetric p-Laplacian problem (2.5) using finite elements on a uniform mesh of step size h. Their experiments suggest that one can usually expect $\mathcal{O}(h)$ convergence in $W^{1,1}(\Omega)$ and $\mathcal{O}(h^2)$ convergence in L^∞.

For our convergence tests with $p > 2$, we concentrate on the convergence of the monotone fronts connecting ± 1 in one-dimension since these solutions creates saddle continua. A good check for convergence in one-dimension is to compute the derivative of the
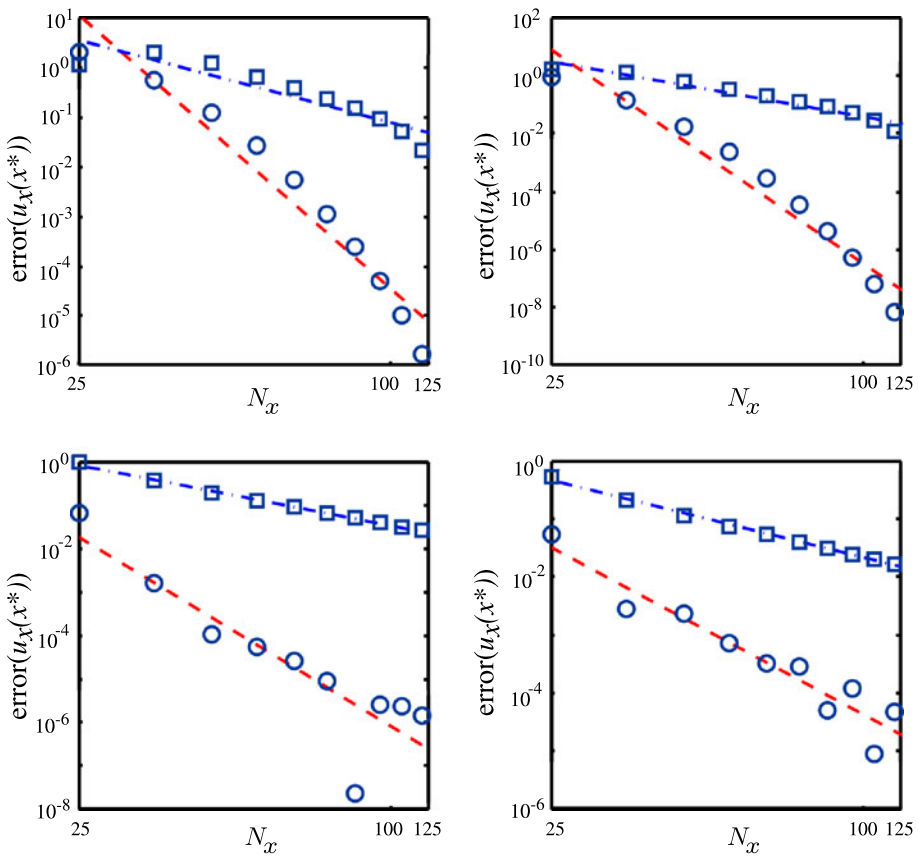
Fig. 3 Finite differences (*squares*) and Chebyshev (*circles*) convergence tests for the one-dimensional bi-stable quasi-linear problem (1.1) with $\varepsilon = 0.1$ and (**a**) $p = 1.75$, (**b**) $p = 2$, (**c**) $p = 3$ and (**d**) $p = 4$. Convergence rates for Chebyshev (*red, dashed lines*) are $\mathcal{O}(N_x^{-9.17})$, $\mathcal{O}(N_x^{-12.27})$, $\mathcal{O}(N_x^{-7.26})$ and $\mathcal{O}(N_x^{-4.79})$ respectively, whereas convergence rates for finite differences (*blue, dash-dotted lines*) are $\mathcal{O}(N_x^{-2.74})$, $\mathcal{O}(N_x^{-3.16})$, $\mathcal{O}(N_x^{-2.31})$ and $\mathcal{O}(N_x^{-2.24})$ respectively

front-type solutions at the point x^* such that $u(x^*) = 0$, and compare with the analytical result

$$u_x(x^*) = \frac{1}{\varepsilon} p'^{1/p}, \qquad (2.7)$$

where $1/p + 1/p' = 1$. This convergence test is carried out in Fig. 3(c) and 3(d) for the Chebyshev discretisation where we see that the Chebyshev method achieves good convergence $\mathcal{O}(N^{-4})$ for relatively small number of modes $N = N_x = N_y = 51$. Finite differences methods appear to be less successful: the error obtained with finite differences is always above 10^{-4} with 10^3 mesh points, whereas Chebyshev error goes below 10^{-4} for 100 mesh points. We observe that the rate of convergence for both discretization schemes appears to be polynomial.

Since fronts do not exist for $p \leq 2$, we cannot use (2.7) as a convergence check at $x = x^*$ and so we plot the absolute error where we compare solutions with the finest mesh approximation; see Fig. 3(a) and 3(b). Here we observe that while the convergence of the finite

difference scheme is polynomial, the Chebyshev discretization converges exponentially. In all cases, we see convergence of the discretization schemes giving us confidence in our numerical results. However, we see that the Chebyshev discretization scheme is better than the finite-difference scheme for all parameter values we are interested in. Hence, in the following sections we shall only use the Chebyshev discretization.

3 Results

3.1 1D

In this section, we will investigate the String method applied to one-dimensional p-Laplacian problem (1.1). Since all solutions of the one-dimensional (1.1) have been characterised and mapped out by Otta [24], we will be primarily interested in how the String method works in locating the saddle-continua.

    We start by looking at the Laplacian case i.e., $p = 2$ and set $\varepsilon = 0.1$. In Fig. 4, we show the convergence string and the corresponding functions along the string's length. We initialise the string by setting $s(x) = \cos(\pi x)$ and $\tilde{u}_1 \equiv 1$, $\tilde{u}_2 \equiv -1$ in (2.4). The converged string shows a large region of constant energy where we observe that the functions are just spatial translations of the "front" solution of (1.1). The non-trivial saddle solution of (1.3) converges to a front solution as $\varepsilon \to 0$. At $\varepsilon = 0.1$, the solution numerically still looks like a front and due to the Neumann boundary conditions at $x = 0$ and $x = 1$, the solution maybe translated in space creating an anomalous saddle-continua which is due to the numerical approximation of (1.3). Hence, while there is a unique front-type solution satisfying (1.1), the string method appears to superficially to find a saddle continua.

    To demonstrate the String method's ability to locate saddle-continua, we compute the strings for $\varepsilon = 0.2$ and $p = 1.5, 2$ and 3; the strings are shown in Fig. 5. All three computed strings develop a plateau. However, when one looks at the derivative of the energy along the string (calculated via first-order finite-differences), we immediately observe a significant difference between the computed paths, see Fig. 5(b). For $p = 3$, where a saddle-continua exists, we see that the plateau of the string is very flat for a number of points. This property is not seen for the $p = 1.5$ or $p = 2$ strings where the derivative of the "plateau" is only
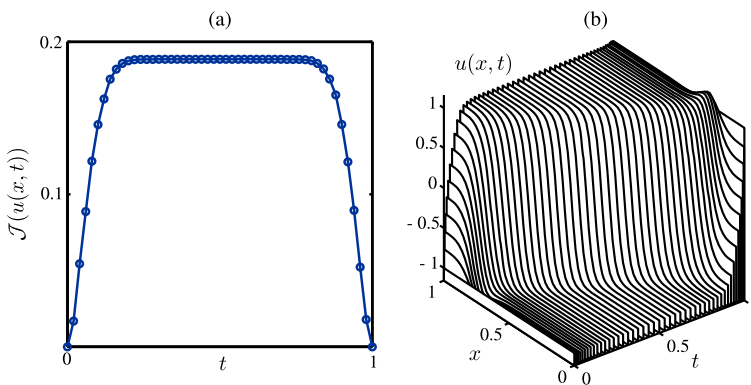

Fig. 4 (**a**) Computed string for $p = 2$, $\varepsilon = 0.1$ with $N_x = 51$, $N_t = 51$. (**b**) Plot of $u(x)$ along the string. We see the flat top of the string in (**a**) corresponds to front-like solutions of (1.1) that are translated in space

Fig. 5 In panel (**a**) we show the computed strings for $\varepsilon = 0.2$ with $N_x = 51$, $N_t = 51$. Panel (**b**) shows the gradient of the energy along the string. Here we see that the String method is able to detect the saddle-continua that exists for $p > 2$. The L^2-norm of the residual is shown in panel (**c**). For $p \geq 2$ we observe excellent convergence of saddle solutions. In panel (**d**) we compute the difference of the strings for $p = 3$ computed using the $H^1(\Omega)$ and $W^{1,p}(\Omega)$-steepest descent
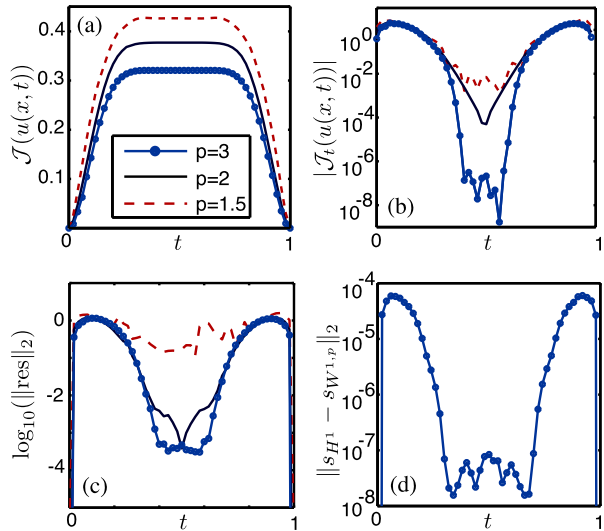
of the order $\sim 10^{-3}$. Points on this plateau for $p > 2$ correspond to solutions of (1.1); see Fig. 5(c). The saddle continua for $p > 2$ is due to the existence of front-type solutions attaining values ± 1 that creates a "dead-core" of solutions where the fronts maybe translated without violating the boundary conditions. These "dead-core" solutions create a continua of critical points of the saddle-point type.

We have found the String method to be particularly poor at finding saddle solutions in the singular diffusion case i.e., $p < 2$; see Fig. 5(c). However, the String method performs very well for $p \geq 2$ and we converge to saddle solutions of (1.1) to within the spatial discretisation error.

We have found no significant difference in the residual or string if we compute with the $H^1(\Omega)$-steepest descent or $W^{1,p}(\Omega)$-steepest descent; see Fig. 5(d). Computationally, there is a considerable advantage in using the $H^1(\Omega)$-steepest descent direction since one only needs to solve a linear system for the steepest descent direction.

We also look at computing other saddle-continua in (1.1) where the solutions re-connect with $u \equiv -1$. To find these types of solutions, we take the string generator $s(x)$ to be

$$s(x) = \tanh(30(x - 0.3)) - \tanh(30(x - 0.7)) - 1. \tag{3.1}$$

Figure 6 shows the string that is computed with the solutions along the string. In this case, the dimension of the manifold of the critical points is two and we find that our String method is only able to detect continua in one of the directions since the computed path is one-dimensional. Further work needs to be carried out to design an algorithm that can compute manifolds of saddle-continua of dimension greater than one.

3.2 2D

In this section, we apply the string and continuation methods to solve equation (1.1) in two spatial dimensions where the numerical shooting method employed by Otta [24] can no longer be applied.

The choice of initial path for the String method has a significant impact on the type of saddles that are located. In Table 1, we detail five possible choices for the initial string
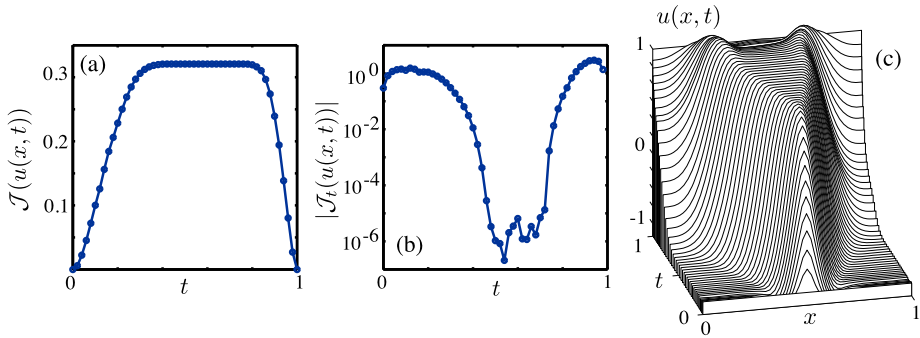
Fig. 6 We show the computed string for $p = 3$, $\varepsilon = 0.1$, $N_x = 51$, $N_t = 51$ with the string generator (3.1). Panel (**a**) shows the energy of the string, (**b**) the gradient of the energy along the string and (**c**) a plot of the solutions along the string. We observe that the plateau of the string is flat to within numerical error

Table 1 Initial string generators s_i leading to saddle solutions u_i of (1.1)

String generator s_i	Nodal domains
$s_1(x, y) = \cos(\pi x)$	two, separated by $x = 0.5$
$s_2(x, y) = \cos(\pi x) - \cos(\pi y)$	two, separated by $y = x$
$s_3(x, y) = \cos(\pi x)\cos(\pi y)$	four, separated by $x = 0.5$ and $y = 0.5$
$s_4(x, y) = \sin(\pi(x + y))\sin(\pi(x - y))$	four, separated by $x = y$ and $y = 1 - x$
$s_5(x, y) = \cos(\pi(x + y))\cos(\pi(x - y))$	five, separated by $|x - 0.5| + |y - 0.5| < 0.5$

generator s_i that connects $\tilde{u}_1 \equiv +1$ to $\tilde{u}_2 \equiv -1$ and classify the generators by the nodal domains of the generator s_i.

In Fig. 7, we first present the saddle-type solutions (determined by the string generator s_i) found by the String method for the Laplacian case $p = 2$. As observed by previous papers [5], the choice of string generator defines the type of saddle solution one finds e.g., the one-dimensional string generator $s_1(x, y) = \cos(\pi x)$ leads to the one-dimensional front-like solutions found in Sect. 3.1.

The Minimum Energy Paths found by the String method using the $H^1(\Omega)$ steepest descent direction for $p = 1.5, 2$, and 3 are shown in Fig. 8 for $\varepsilon = 0.2$; similar MEPs are found for the string generators s_3, s_4 and s_5. All our numerical investigations have failed to find saddle-continua in two dimensions for all the string generators $s_2, \ldots, s_5$. We believe that this lack of saddle-continua is due to the Neumann boundary conditions preventing any translations of the solutions.

4 Conclusion

In this paper, we have developed the String method of [15] for the quasi-linear problem (1.1). The numerical method employed in this paper, allows one also to locate saddle points of $\mathcal{J}$ for domain $\Omega \subset \mathbb{R}^n$, $n > 1$ where the numerical shooting method of Otta [24] can no longer be applied. We have found that the String method naturally produces paths that can locate saddle-continua and provide crucial information on the temporal dynamics of the parabolic
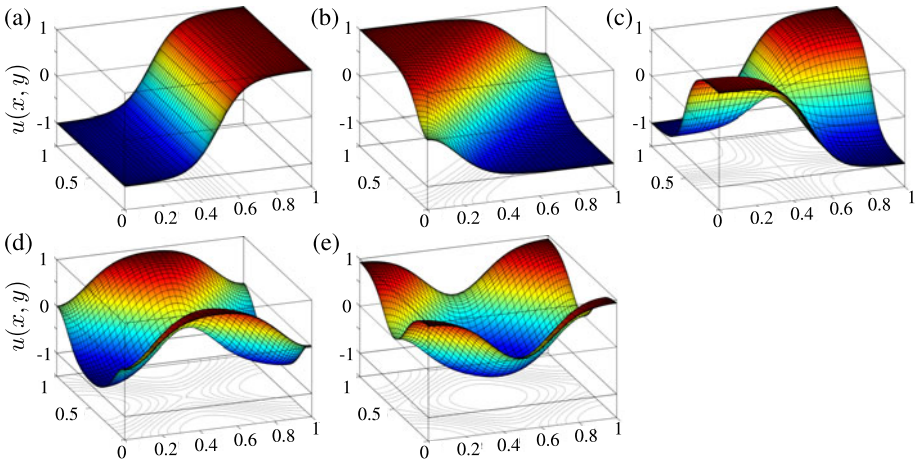
Fig. 7 Saddles solutions of (1.1) with $p = 2$, $\varepsilon = 0.2$, found from the String method with the string generators (**a**) $s_1(x, y)$, (**b**) $s_2(x, y)$, (**c**) $s_3(x, y)$, (**d**) $s_4(x, y)$ and (**e**) $s_5(x, y)$. Computational parameters $N_t = 21$, $N_x = N_y = 51$
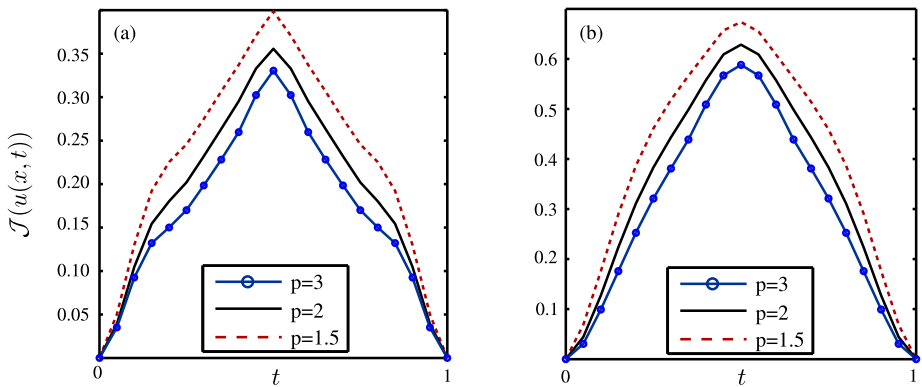

Fig. 8 Minimum energy paths for (1.1) with (**a**) $\varepsilon = 0.1$ and (**b**) $\varepsilon = 0.2$ for $p = 1.5$, 2, and 3. Computational parameters $N_t = 21$, $N_x = N_y = 51$ with the string generator $s_2(x, y)$

p-Laplacian problem (1.5). However, we were unable to locate any saddle-continua in two dimensions.

Our computations suggest there is no computational benefit to carrying out the steepest descent direction in the general $W^{1,p}(\Omega)$ space. However, it is not clear that this holds for general quasi-linear PDEs. In our opinion, the String method is significantly more robust than the standard saddle-locating algorithm [5] since it naturally carries out re-meshing along the path and minimises the energy of every point along the path.

The numerical methods discussed in Sect. 2, can easily be extended to the general quasi-linear problem

$$-\nabla \cdot (r(x)\varphi(\nabla u(x))) + g(x, u(x)) = f(x), \quad x \in \Omega, \tag{4.1}$$

where $g \in \mathrm{CAR}(\Omega, \mathbb{R}), r(x) > 0, \forall x \in \Omega, f \in L^{p'}(\Omega)$, and φ is strictly increasing, homogeneous function on $\mathbb{R}$.

Our work revealed some directions for future research. Since the String method finds a stationary path of (2.1), it could be interesting to use path-following techniques to continue the minimum energy path in p and ε. Also an open question is the proof of optimal convergence results for the Chebyshev discretization scheme since this type of discretisation scheme seems to be significantly better than the standard 5-point finite-element discretisation. Finally, to the best author's knowledge there were no attempts to prove that saddle-continua do or do not exist in higher-dimensional quasi-linear problem (1.1).

References

1. Alikakos, N., Bates, P.W., Fusco, G.: Slow motion for the Cahn-Hilliard equation in one space dimension. J. Differ. Equ. **90**, 81–135 (1991)
2. Ambrosetti, A., Rabinowitz, P.H.: Dual variational methods in critical point theory and applications. J. Funct. Anal. **14**, 349–381 (1973)
3. Barrett, J.W., Liu, W.B.: Finite element approximation of the p-Laplacian. Math. Comput. **61**, 523–537 (1993)
4. Budd, C.J., Huang, W., Russell, R.D.: Adaptivity with moving grids. Acta Numer. **18**, 111–241 (2009)
5. Choi, Y.S., McKenna, P.J.: A mountain pass method for the numerical solution of semilinear elliptic problems. Nonlinear Anal. **20**, 417–437 (1993)
6. Chow, S.-S.: Finite element error estimates for nonlinear elliptic equations of monotone type. Numer. Math. **54**, 373–393 (1989)
7. Coleman, T.F., Li, Y.: A reflective Newton method for minimizing a quadratic function subject to bounds on some of the variables. SIAM J. Optim. **6**, 1040–1058 (1996)
8. Costa, D.G., Ding, Z., Neuberger, J.M.: A numerical investigation of sign-changing solutions to superlinear elliptic equations on symmetric domains. J. Comput. Appl. Math. **131**, 299–319 (2001)
9. DiBenedetto, E.: $\mathcal{C}^{1+\alpha}$ local regularity of weak solutions of degenerate elliptic equations. Nonlinear Anal. **7**, 827–850 (1983)
10. Ding, Z., Costa, D., Chen, G.: A high-linking algorithm for sign-changing solutions of semilinear elliptic equations. Nonlinear Anal. **38**, 151–172 (1999)
11. Drábek, P., Manásevich, R.F., Takáč, P.: Manifolds of critical points in a quasilinear model for phase transitions. Contemp. Math., Nonlinear Elliptic Part. Differ. Equ. **540**, 95–135 (2009, in preparation)
12. Drábek, P., Milota, J.: Applications to differential equations. In: Methods of Nonlinear Analysis. Birkhäuser Advanced Texts: Basler Lehrbücher. [Birkhäuser Advanced Texts: Basel Textbooks]. Birkhäuser, Basel (2007)
13. E, W., Ren, W., Vanden-Eijnden, E.: String method for the study of rare events. Phys. Rev. B **66**
14. E, W., Ren, W., Vanden-Eijnden, E.: Energy landscape and thermally activated switching of submicron-sized ferromagnetic element. J. Appl. Phys. **93**
15. E, W., Ren, W., Vanden-Eijnden, E.: Simplified and improved string method for computing the minimum energy paths in barrier-crossing events. J. Chem. Phys. **126**
16. Fusco, G., Hale, J.K.: Slow-motion manifolds, dormant instability, and singular perturbations. J. Dyn. Differ. Equ. **1**, 75–94 (1989)
17. Glowinski, R., Marrocco, A.: Sur l'approximation, par éléments finis d'ordre un, et la résolution, par pénalisation-dualité, d'une classe de problèmes de Dirichlet non linéaires. RAIRO. Anal. Numér. **9**, 41–76 (1975)
18. Henkelman, G., Jóhannesson, G., Jónsson, H.: Methods for finding saddle points and minimum energy paths. In: Schwartz, S.D. (ed.) Progress on Theoretical Chemistry and Physics, pp. 269–300. Kluwer Academic, Dordrecht (2000)
19. Krauskopf, B., Osinga, H.M., Galan-Vioque, J. (eds.): Numerical Continuation Methods for Dynamical Systems. Springer, Berlin (2007)
20. Kuzin, I., Pohozaev, S.: Entire Solutions of Semilinear Elliptic Equations. Birkhäuser, Basel (1997)

21. Li, Y., Zhou, J.: A minimax method for finding multiple critical points and its applications to semilinear PDEs. SIAM J. Sci. Comput. **23**, 840–865 (2001) (electronic)
22. Modica, L.: The gradient theory of phase transitions and the minimal interface criterion. Arch. Ration. Mech. Anal. **98**, 123–142 (1987)
23. Oruganti, S., Shi, J., Shivaji, R.: Diffusive logistic equation with constant yield harvesting. I. Steady states. Trans. Am. Math. Soc. **354**, 3601–3619 (2002) (electronic)
24. Otta, J.: Analysis of the quasilinear bi-stable equation. To appear (2009)
25. Otta, J.: Analysis of the quasilinear bi-stable equation (2009, to appear)
26. Qian, T., Ren, W., Sheng, P.: Current dissipation in thin superconducting wires: accurate numerical evaluation using the string method. Phys. Rev. B **72**
27. Qiu, C., Qian, T., Ren, W.: Phase slips in superconducting wires with nonuniform cross section: a numerical evaluation using the string method. Phys. Rev. B **77**
28. Russell, R.D., Christiansen, J.: Adaptive mesh selection strategies for solving boundary value problems. SIAM J. Numer. Anal. **15**, 59–80 (1978)
29. Struwe, M.: Applications to nonlinear partial differential equations and Hamiltonian systems. In: Variational Methods, 3rd edn. Ergebnisse der Mathematik und ihrer Grenzgebiete. 3. Folge. A Series of Modern Surveys in Mathematics [Results in Mathematics and Related Areas. 3rd Series. A Series of Modern Surveys in Mathematics], vol. 34. Springer, Berlin (2000)
30. Trefethen, L.N.: Spectral Methods in MATLAB. Software, Environments, and Tools, vol. 10. SIAM, Philadelphia (2000)
31. Truhlar, D.G., Garrett, B.C., Klippenstein, S.J.: Current status of transition-state theory. J. Phys. Chem. **100**, 12771–12800 (1996)